Ganoderma lucidum polysaccharide loaded sodium alginate micro-particles prepared *via* electrospraying in controlled deposition environments

Zhi-Cheng Yao[a,b], Li-jie Jin[a,b], Zeeshan Ahmad[c], Jie Huang[d], Ming-Wei Chang[a,b,*], Jing-Song Li[a]

[a] Department of Biomedical Engineering, Key Laboratory of Ministry of Education, Zhejiang University, Hangzhou 310027, People's Republic of China.

[b] Zhejiang Provincial Key Laboratory of Cardio-Cerebral Vascular Detection Technology and Medicinal Effectiveness Appraisal, Zhejiang University, Hangzhou 310027, People's Republic of China.

[c] Leicester School of Pharmacy, De Montfort, University, The Gateway, Leicester, LE1 9BH, UK.

[d] Department of Mechanical Engineering, University College London, London WC1E 7JE, UK.

*corresponding author: Ming-Wei Chang, Ph.D., Assoc. Professor

Tel: +86(0)571-87951517, Email: mwchang@zju.edu.cn

ABSTRACT

Ganoderma lucidum polysaccharide (GLP) is a functional food source deployed in preventative medicine. However, applications utilizing GLP are limited due to oxidative and acidic environmental damage. Advances in preserving GLP structure (and therefore function), *in situ,* will diversify their applications within biomedical fields (drug and antibacterial active delivery *via* the enteral route). In this study, GLP loaded sodium alginate (NaAlg) micro-particles (size range 225-355 μm) were generated using the electrospray (ES) process. The loading capacity and encapsulation efficiency of GLP for composite particles (collected at different temperatures) were ~23% and 71%, respectively. The collection substrate ($CaCl_2$, 1-20 w/v %) concentration was explored and preliminary findings indicated a 10 w/v % solution to be optimal. The process was further modified by manipulating the collection environment temperature (~25 to 50 °C). Based on this, NaAlg/GLP micro-particles were engineered with variable surface morphologies (porous and crinkled), without effecting the chemical composition of either material (GLP and NaAlg). *In-vitro* release studies demonstrated pH responsive release rates. Modest release of GLP from micro-particles in simulated gastric fluid (pH~1.7) was observed, while rapid release was exhibited under simulated intestinal conditions (pH~7.4). Release of GLP from NaAlg beads was the greatest from samples prepared at elevated environmental temperatures. These findings demonstrate a facile route to fabricate GLP-NaAlg loaded micro-particles with various shapes, surface topographies and release characteristics *via* a one-step ES process.

Key words: Encapsulation; Temperature regulation; Food; Cross-Linking; Oral.

1. Introduction

Ganoderma lucidum (GL) is a basidiomycete white rot fungus belonging to the *Aphyllophorals* family. It has been deployed in preventative medicine for more than 2000 years (Ma et al., 2015). The benefits of GL have been documented in several studies; as a potential therapy for hepatitis, chronic bronchitis, gastritis, various tumors and immunological disorders. The fungus also displays anti-neoplastic, anti-inflammatory, antioxidant and immune-regulation properties (Ma et al., 2013; Zhang et al., 2016). The main bioactive substances associated with GL are polysaccharide and triterpenes; which are easily isolated from fruit bodies, mycelia and spores (Pan et al., 2013). Several reports indicate *Ganoderma lucidum* polysaccharide (GLP) to exhibit the aforementioned properties (Shi et al., 2013; Wang et al., 2009), while several other studies show GLP's potential in other global healthcare challenges (Jie et al., 2009; Shi et al., 2013; Teng et al., 2012). *In-vivo* experiments utilizing GLP exhibit little to no toxicity (Zhang et al., 2016), implying their relatively high biocompatibility. Despite these benefits, β-D-glucan (a form of polysaccharide isolated from GL) is extremely sensitive to oxidative degradation (including the reactions of active oxygen substances e.g. hydroxyl radicals). This environmental damage is most likely to occur during the storage process and subsequently limits GLP efficacy (Kivelä et al., 2012). Hence, it is essential to protect GLP after its extraction from GL and post formulation in order to preserve function. This limited longevity has impeded its potential use in the pharmaceutical arena.

Sodium alginate (NaAlg) is a natural polysaccharide comprising D-mannuronic and L-gulunronic acids, and is commonly extracted from marine brown algae (Hamid et al., 2008). NaAlg has been widely used as an encapsulating matrix material because

of cost effectiveness, process ability and biocompatibility. Ionic cross-linking is used to yield three dimensional structures which reduces undesirable interactions between encapsulated moieties and external environmental factors (e.g. oxidizing agents and UV light) (Iliescu et al., 2014). Moreover, because of NaAlg's ionic nature, the release of encapsulated materials can be controlled based on external pH environments. In acidic conditions (pH ~2) release is retarded, whereas enhanced release is observed at more neutral pH values (~6 to 8) (Zhao et al., 2016). For these reasons, several studies utilizing NaAlg have focused on protective and controlled release functions using encapsulated oils (e.g. peppermint (Koo et al., 2014)) and viruses (e.g. adenovirus) *via* cross-linked beads (Park, 2012).

The electrospray (ES) technique is a one-step preparation method which has been widely used to engineer particles ranging from tens of nanometers to hundreds of micrometers (Gao et al., 2016). The diameter and surface morphology of generated particles is regulated by process parameter manipulation (e.g. flow rate, applied voltage and collector distance) (Yuan et al., 2016). In addition, the process has been used to fabricate particles with varied surface topographies through vapor-induced phase separation (Meng et al., 2009), non-solvent collecting mediums (Gao et al., 2014) selective coating layers (Yao et al., 2016b) and by altering the environmental humidity and polymer molecular weight (Casper et al., 2003; Wu and Clark, 2007). Interestingly, topographical and surface area-to-volume ratios (arising from particle shape) have been shown to impact active release from an embedded matrix (Gao et al., 2015). This provides a shape driven drug delivery approach, although the effect of environmental process temperature at the site of ES deposition on particle shape and

surface topography is limited. This is crucial since the ES process is an atomization method and therefore solvent vaporization effects need to be explored further.

In this study, we demonstrate two aspects relating to GLP encapsulation which have potential to enable its pharmaceutical function and suitability. Firstly, a new combination of process (electrospray) and materials (GLP and NaAlg) is shown incorporating optimization and the demonstration of a crucial process factor (i.e. the environmental process temperature). This is an important find for electrohydrodynamic processing using this material, but also very relevant to other pharmaceutical technologies which deploy elevated or variable temperatures for particle engineering. Secondly, directly linked to this process parameter, particle morphology and release dynamics of GLP from microcapsules are varied; providing a route to modulate such properties during an unexplored engineering step. Since the particle size is coarse and comparable in dimension to systems deployed for oral delivery, GLP release behavior is shown over a pH range; typical of what is expected at selected points in the GI tract once administered orally.

2. Materials and methods

2.1. Materials

Sodium alginate (NaAlg, A1112) and calcium chloride dehydrate ($CaCl_2$, C4901) were purchased from Sigma Aldrich (St. Louis, Mo., USA). Phosphate buffer solution (PBS) was obtained from Sinopharm Chemical Reagent Co., Ltd (Shanghai, China). Deionized water was produced using a Millipore Milli-Q Reference ultra-pure water purifier (USA). High purity-grade wood-log cultivated GLS and commercial broken

spore products were obtained from TianHe Agricultural Group (Zhe Jiang Long Quan, China). All chemicals used were analytical grade without additional purification.

2.2. Extraction of GLP from Ganoderma Lucidum spores

Ganoderma Lucidum spore powder was added to DI water to prepare a 5 w/v% mixture. The mixture was subjected to ultrasound irradiation (υ=40 kHz) by using an ultrasonic device (KS-300 EI, Kesheng Co., Ltd, Zhejiang, China) for 50 min at 70°C, followed by centrifugation for 15 min at 12000 rpm. The supernatant was then removed and stored. The process was repeated three times by further additions of DI water (to make up to the primary volume) followed by ultrasound and centrifugation. All (stored) supernatant was placed into a flask and then rotary distillated (50°C). The resulting sample was freeze dried which yielded solid polysaccharide.

2.3. Preparation of electrospraying solutions

Pure NaAlg solution (2 w/v%) was prepared by dissolving NaAlg powder into DI water. GLP was then added into the 2 w/v% NaAlg solution at a ratio of 2:1 (weight of NaAlg solute : weight of GLP) to achieve a homogeneous mixture. Known quantities of $CaCl_2$ were dissolved into DI water to prepare several $CaCl_2$ solutions (1, 2, 5, 10, and 20 w/v%), which were subsequently used as collection mediums. A magnetic stirrer (VELP ARE heating magnetic stirrer, Italy) was used to achieve complete dissolution of the powder. The solutions were individually mechanically stirred at ~300 rpm at ambient temperature (25°C) for 1 h.

2.4. Fabrication of electrosprayed micro-particles

Micro-particles were fabricated using the ES technique as illustrated in **Fig. 1a**. The set-up includes a high power voltage supply, a high-precision syringe pump, a stainless steel needle and a ring-shaped ground electrode. The formulated liquid was propelled by a syringe pump (KD Scientific KDS100, USA) into the metallic needle (the inner and outer diameters were 0.8 mm and 1 mm, respectively) using a feeding rate range between 6.0 to 10.0 mL/h. An electric field was applied (Glassman high voltage Inc. series FC, USA), and the voltage ranged from 14.0 to 16.0 kV. Selected $CaCl_2$ solution (collector medium) was placed directly below the metallic needle at a distance of 500 mm, while the ground electrode was set at 150 mm below the needle orifice. For each condition, a collection time of 2h was deployed which enabled sufficient particle collection for further analysis. During the ES process, the environment temperature was controlled using a heating apparatus (FH-06A, Liqi electric appliance Co., Ltd, Zhejiang, China) and temperature readings were observed around the collection area to ensure uniformity. A high-speed camera (Baummer TXG02C, Germany) was used to observe ES jetting modes. Collected micro-particles were dried prior to further analysis using an electric vacuum drying oven (D2F-6020AF, Gongxing Laboratory Instrument Co., Ltd, Tianjin, China) at a pressure of 0.1 MPa (25 °C) for 24 h.

2.5. Particle morphology assessment

Optical (OM, Pheonix BMC503-ICCF, China) and field emission scanning electron microscopy (SEM, SU 8000 SEM, Hitachi, Japan) were used to study the size distribution and surface morphology of generated micro-particles. For SEM analysis, an accelerating voltage of 20 kV was used to obtain micrographs. Samples were fixed on metallic stubs by double-backed conductive tape. Prior to analysis, all samples

were sputter-coated (Ion sputter MC 1000, Hitachi, Japan) with a thin layer of gold under vacuum for 60 s using a current intensity of 25 mA. Particle size distribution (collected at various process conditions) was obtained using electron micrographs and ImageJ software (National Institute of Health, MD, USA). Aspect ratio was used to determine micro-particle shape, and was calculated using Equation (1):

$$Aspect\ ratio\ (\%) = \frac{Width\ of\ bead\ (\mu m)}{Length\ of\ bead\ (\mu m)} \times 100\% \qquad (Eq.1)$$

For each sample, 100 random particle diameters were assessed, and the mean was obtained.

2.6. Fourier transform infrared spectroscopy

Fourier Transform Infrared (FTIR) spectroscopy (IR Affinity 1, Shimadzu, Japan) was used to determine the presence of materials, chemical interactions and material stability. Samples were prepared using the KBr pellet pressing method, and a scanning range of 4000-400 cm^{-1} was used. 2 mg of each sample (pure NaAlg powder, pure GLP, and NaAlg/GLP particles collected at different temperatures) was blended with 200 mg KBr powder by grinding in a mortar. The resulting mixture was then pressed into transparent pellets under a pressure of ~20 MPa. Spectra were obtained using 20 scans per sample.

2.7. Loading capacity and encapsulation efficiency of GLP

For the cross-linking procedure, encapsulated GLP-NaAlg particles were collected into $CaCl_2$ solution. During this process, quantities of GLP may have transferred into $CaCl_2$ medium. Therefore, the GLP content in $CaCl_2$ medium was used to determine LC and EE. The method of determining LC and EE was adapted according to

previously reported methods (Chatterjee and Judeh, 2015; Moomand and Lim, 2014). The loading capacity (LC) of GLP is the quantity of GLP encapsulated within NaAlg matrix, and was calculated using Equation (2):

$$LC\ (\%)=\frac{Amount\ of\ GLP\ content\ entrapped\ in\ the\ particles\ (\mathrm{mg})}{Weight\ of\ the\ micro\text{-}particle\ (\mathrm{mg})}\times 100\% \qquad (\mathrm{Eq.2})$$

Un-encapsulated polysaccharide is prone to dissolution in $CaCl_2$. Thus, the encapsulation efficiency (EE) of GLP within NaAlg micro-particles was determined using Equation (3):

$$EE\ (\%)=\frac{Amount\ of\ GLP\ content\ entrapped\ in\ the\ particles\ (\mathrm{mg})}{Theoretical\ total\ amount\ of\ GLP\ (\mathrm{mg})}\times 100\% \qquad (\mathrm{Eq.3})$$

The quantity of GLP entrapped in NaA1g was determined by calculating the difference between the total quantity of GLP added into the NaAlg matrix and the GLP residue quantity in the collector medium ($CaCl_2$ solution) (Li et al., 2013). The GLP content in $CaCl_2$ solution was determined by measuring absorbance at 221 nm (the characteristic UV-Vis absorption of GLP) in triplicate using a UV-2600 spectrophotometer (Shimadzu, Japan) (Qiu et al., 2001).

2.8. In vitro release measurement

GLP release from NaA1g matrices was assessed to evaluate the effect of process parameter modulation during ES particle synthesis. NaAlg/GLP particles were assessed in simulated gastric fluid (SGF, pH=1.7, prepared using HCl solution) for 2 h, and were then removed and added to simulated intestinal fluid (SIF, pH=7.4, prepared using 0.02 M phosphate buffer) for a further 4 h. For this, approximately 100 mg of NaAlg/GLP micro-particles (engineered using various collection environment

temperatures; 25, 35 and 50 °C) were placed into 10 mL of selected GIT medium (SGF of SIF) and incubated at 37 °C. At designated time intervals, 2 mL of supernatant was removed from the assessment medium and replaced with an equal volume of fresh release medium. The withdrawn samples were filtered (0.45 μm Millipore) before UV-Spectrophotometric analysis. GLP concentration in the supernatant was measured using a wavelength of 221 nm (Fu et al., 2009). The percentage of GLP released was calculated using Equation (4) (Qiu et al., 2001):

$$GLP\ release\ (\%) = \frac{Q_t}{Q_s} \times 100\% \qquad \text{(Eq.4)}$$

Here, Q_t is the quantity of GLP released at time t, Q_s is the total quantity released

2.9. Statistical analysis

All experiments were performed in triplicate and data is presented as mean±standard deviation (n=3). Statistical analysis was performed using SPSS software (SPSS Statistics v18, IBM, UK). Statistically significant differences between variables were assessed *via* one-way analysis of variance (ANOVA) followed by student's t-Test (*$p<0.05$). All statistical data were plotted using Origin software (OrginLab, USA).

3. Results and discussion

3.1. Fabrication of NaAlg/GLP micro-particles

GLP is known to exhibit beneficial antioxidant properties with potential applications in several biomedical spheres. These, however, become compromised due to rapid environmental damage. GLP function is linked to its structure and encapsulation provides an opportunity to preserve these functions by limiting environmental interaction. The preparation of NaAlg/GLP composite (encapsulated) micro-particles

was achieved using the ES process. When conventional process parameters (flow rate, collector distance and physical properties of formulation media) are constant, the applied voltage was determined to be the most dominant factor in the ES particle engineering process. Optimizing the applied voltage caused the liquid meniscus at the needle orifice to deform into the preferred conical shape, forming a cone-jet. **Fig. 1b** shows the dripping mode at zero electrical potential, which is due to gravitational force and mechanical syringe action. When the applied voltage reached 15 kV, the stable jetting mode was observed, as shown in **Fig. 1c**.

3.2. Effect of collector medium concentration

A series of $CaCl_2$ solutions (ranging in 1-20 w/v %) was used for the cross-linking process during collection of NaAlg particles. The concentration of cross-linking agent is essential for spherical bead formation, at low $CaCl_2$ concentrations NaAlg particles aggregate and lead to clump formation (Ghayempour and Mortazavi, 2013). **Figs. 2a-g** show NaAlg particles collected using different $CaCl_2$ concentrations, while the gelation time for all samples in $CaCl_2$ solution was kept constant (2 h). **Fig. 2a** shows droplets deposited without any $CaCl_2$ substrate (0 w/v%), while NaAlg particles collected in low $CaCl_2$ concentration's (0.5 w/v %) presented anomalous shapes due to insufficient crosslinking (**Fig. 2b**). At all concentrations from 1-20 w/v%, particles were formed with spherical morphologies, indicating interaction between $CaCl_2$ collection medium and NaAlg sprayed droplets (transitioning into particles). The mean diameter (**Fig. 2h)**, of NaAlg particles decreased, with increasing $CaCl_2$ concentration. The mean diameters of NaAlg particles were 356.4±30.4, 334.0±53.6, 313.0±50.9, 303.4±15.2, and 303.6±29.5 μm, and were prepared using 1, 2, 5, 10, and 20 w/v% $CaCl_2$, respectively. This is due to the increased quantity of Ca^{2+} ions at

higher $CaCl_2$ concentration, which leads to instantaneous cross-linking. The impact of Ca^{2+} ion concentration on particle size does reach a threshold as there is little difference in particle diameter between those collected using 10 and 20 w/v% $CaCl_2$ solutions. In addition, NaAlg beads prepared using high $CaCl_2$ concentrations also impact release kinetics of encapsulated materials (Huang et al., 2012). Therefore, 10 w/v% $CaCl_2$ solution was selected for further experimentation involving NaAlg/GLP micro-particles for controlled active release and assessment.

In our study, a collection time of 2h was deployed to obtain sufficient particles for further analysis. Optical micrographic comparison for optimal structures collected (in $CaCl_2$) at <1 minute and 30 minute post-collection, show no change to the particle size. This also negates any suggestion of size change arising from uptake of the deposition medium.

3.3. Effect of various ES process parameters on particle size

Flow rate is also a significant ES parameter in particle size modulation. The effect of flow rate on particle diameter was investigated by manipulating the liquid feed rate (6.0, 7.0, 8.0, 9.0, and 10.0 mL/h), while all other ES parameters were kept constant (collector distance: 500 mm and applied voltage: 15 kV). **Figs. 3a&b** show the relationship between mean particle diameter distribution (for both pure NaAlg and composite NaAlg/GLP particles) and media infusion rate. At a flow rate of 6.0 mL/h, mean particle diameters of NaAlg/GLP and NaAlg particles were 242.5±8.5 and 234.9±16.4 μm, respectively. When the flow rate is increased to 10.0 mL/h the resulting mean particle diameter increases (279.4±13.2 and 277.6±13.7 μm, respectively). In addition, pure NaAlg particles exhibit a broader particle diameter

range across various flow rate assessments which is attributed to the formulation's (infusion medium's) lower viscosity. The effect of voltage on particle size distribution was assessed based on an applied voltage range of 14.0 to 16.0 kV. In this instance, media flow rate was maintained at 8.0 mL/h and the deposition distance was fixed at 500 mm. The relationship between applied voltage and mean particle diameter is presented in **Figs. 3c&d**, exhibiting inverse correlation. For example, at 14.0 kV mean diameters of NaAlg/GLP and NaAlg particles were 297.9±14.4 and 297.3±18.7 μm, while at 16.0 kV these decreased to 228.3±14.2 and 225.9±14.2 μm, respectively. This difference is due to enhanced electrostatic repulsive force on the fluid jet arising at greater electric fields. An increase in columbic force is also expected which facilitates a reduction in the mean particle diameter (Bhardwaj and Kundu, 2010).

To determine the effect of collection distance on micro-particle formation, the distance between the processing orifice and collecting medium surface ($CaCl_2$ solution) was systematically varied from 300 to 500 mm. In this instance, media flow rate and applied voltage were constant (10.0 mL/h and 15.0 kV, respectively). An inverse relationship between mean particle diameter and collection distance is observed. When needle outlet to collecting medium distance is fixed at 300 mm, the mean NaAlg/GLP and NaAlg particle diameters were 291.1±29.8 and 307.4±39.6 μm, respectively. Increasing this distance further to 500 mm leads to a reduction in mean particle diameter (241.6±17.1 and 237.6±18.1 μm, respectively). This change is attributed to solvent volatilization (i.e. DI water), which increases with the distance a droplet has to travel. This leads to reduced water content within the forming particle (in the NaAlg matrix) after cross-linking yielding smaller particles (Yuan et al., 2016). In addition, a greater collection (or deposition) distance also causes NaAlg/GLP bead

elongation (Zhao et al., 2016). Therefore, in order to prepare near-uniform micro-particles, a collection distance of 500 mm was selected for further experiments. The broader size distribution of NaAlg particles (as a function of collection distance), compared to the composite system, is attributed to a lower viscosity of the parent formulation (infusion medium).

3.4. Effect of temperature on particle morphology and structure

A heating apparatus was used to regulate and control the environmental temperature (measured at several points under the ES nozzle to the collection substrate) during the ES process. Three temperatures were selected; 25 °C (ambient), 35 °C (warm) and 50 °C (high) and particles were collected under each environment. NaAlg/GLP particle structure, size and morphology differed in all conditions. **Fig. 4** presents optical micrographs and particle size distributions of composite beads collected under the three environments. Formulations sprayed into a 50 °C environment yield particles with reduced diameters (223.1±15.3 μm). Particles formed at 25 and 35 °C possess mean diameters of 270.4±10.9 and 238.6±16.9 μm, respectively. This is attributed to enhanced solvent evaporation at greater environmental temperatures, which interplays with residual water content in the particle system prior to cross-linking in $CaCl_2$ solution (collection medium). Furthermore, the shape of NaAlg/GLP micro-particles is also affected during temperature modulated synthesis (**Fig. 4e**), with beads obtained at 50 ºC and deformed-elongated particles at the ambient temperature (**Fig. 4a**) (Bhardwaj and Kundu, 2010; Mckee et al., 2004).

Composite and pure particle (NaAlg) surface topography is shown in **Fig. 5.** Near uniform, speherical NaAlg micro-particles were successfully obtained at 25 °C (**Fig.**

5a), and their aspect ratio is 93.1±3.8% (**Fig. 5c**). Closer inspection *via* electron microscopy (**Fig. 5b**) revealed crinkled particle surface topography. However, as shown in **Fig. 5d**, electrospraying of composite formulation in a 25 °C environment yielded conical shaped particles possessing extensive nano-scaled cavities on their surface (**Fig. 5e**), with appreciable variation to the aspect ratio (74.6±9.3%). Electrospraying the identical composite formulation (NaAlg/GLP) in a 35 °C environment leads to a change in particle geometry; with particles appearing more spherical with an increased aspect ratio of 87.9±6.8% (schematic diagrams presented in **Figs. 5f, i, &l**). The crinkled particle surface morphology becomes more prominent with a rise in the environmental temperature (**Fig. 5h**). At the greatest electrospraying environmental temperature (50 °C) resulting particles appear trenched with a clearly pronounced corrugated topography (**Fig. 5k**). These variations are directly linked to the degree of solvent evaporation from the perfused solution and its viscosity.

FTIR spectroscopy was used to affirm the presence of chemical composition, material degradation and any possible interactions between encapsulated GLP and the NaAlg matrix. **Fig. 6** shows the infrared spectra of pure NaAlg powder, GLP and the electrosprayed NaAlg/GLP composite particles collected at different environmental temperatures (25, 35 & 50 °C). For pure NaAlg powder, the peak at 1635 cm^{-1} corresponds to the ester linkage stretching (Ribeiro et al., 2004). Constituents of GLP are also detected. Characteristic peaks corresponding to C-N stretching (amine groups within polysaccharide) are found at 1035, 1079, and 1436 cm^{-1} (Qin and Wun, 2002; Wang et al., 2012). Characteristic peak intensity of GLP was relatively low in the NaAlg/GLP composite particle spectrum, which is due to the reduced GLP content as the system also comprises NaAlg. By comparing the five spectra (**Fig. 6)**, characteristic peaks of NaAlg and GLP exhibit no obvious variation indicating the

successful encapsulation of GLP in NaAlg matrix using the ES process. Moreover, the results indicate the heating process does not lead to any structural or chemical change to GLP and NaAlg.

3.5. GLP loading and release

Compared to other encapsulation techniques, such as dispersion and emulsification, the ES process is an efficient and economical route to load, encapsulate and engineer particles in a single step (Koo et al., 2014; Yao et al., 2016a). The influence of environmental electrospraying temperature on GLP loading within the NaAlg matrix (LC) and the encapsulation efficiency (EE) were measured. LC indicates the quantity of GLP encapsulated within the NaAlg particle matrix per unit weight, while EE is the efficiency of the ES process for retaining GLP within the particle structure. The LC of GLP within NaA1g is 23.4±1.0, 23.3±1.0 and 23.6±1.2% at 25, 35 and 50 °C (**Fig. 7**), respectively, indicating no noticeable impact of temperature. The EE values of GLP within the matrix collected at 25, 35, 50 °C are 71.9±1.1, 70.1±1.0 and 70.6±1.6%, respectively, which also suggest little to no impact arising from the environmental temperature. These results demonstrate the valuable role of environmental temperature during the ES process on regulating particle shape and morphology without interfering with drug loading or encapsulation efficiency.

Variation in particle size distribution, surface morphology and topography has a clear impact on GLP release. The pH environment across the GIT varies from acidic (gastric) to neutral-alkali (intestinal). The pH value of gastric fluid ranges from 1 to 3, while that of the intestine is almost neutral (Lazaridou and Biliaderis, 2007). In order to replicate the digestion process *in-vitro*, the release of GLP from the particle matrix

system was assessed by incubating electrosprayed composite particles in SGF for 2 hours followed by incubation in SIF for a further 4 hours. **Fig. 8** shows release profiles of GLP from encapsulated NaAlg composite beads prepared under different environmental temperatures (25, 35 and 50 °C). GLP release in SGF (pH 1.7) over the 2 hour *in vitro* period was slow. Approximately 1.3, 1.0 and 1.0% was released from the NaAlg/GLP matrix particle systems formed at 25, 35 and 50 °C, respectively. This release behavior is in agreement with earlier findings relating to NaAlg matrices (Huang et al., 2012). Here, a contraction of polymeric chains is caused by the unionization of carboxylic acid groups when the pH of the incubation medium is below the p*K*a of NaAlg (3.2-4); this leads to reduced electrostatic repulsion (Zhao et al., 2016). Thus, GLP was preserved and retained within the NaAlg matrix, presenting a potential way for preventing denaturation in the acidic SGF environment.

In contrast, GLP release in SIF is much quicker. An increase in the surrounding pH causes carboxylic acid groups to ionize, thereby increasing electrostatic repulsion and polymer chain relaxation thus providing greater motility of encapsulated GLP (Wee and Gombotz, 1998). The release of GLP increases to 81.6%, 96.3%, and 96.5% (for particles prepared at 25, 35 and 50 °C environments, respectively) post 45 minutes incubation (time point of 2.75 h in **Fig. 8**). The release of GLP continues steadily with incubation time (up to 3 h). Release of GLP from composite beads (in SIF) prepared at various ES environmental temperatures also exhibited distinct differences. Approximately 90% of encapsulated GLP was released at t=120, 35 and 25 min for particles formed at 25, 35 and 50 °C, respectively. This is due to individual topographic features of NaAlg/GLP particles. As shown previously in **Fig. 5e**, composite particles collected at 25 °C were less porous than those engineered at 35 and 50 °C (**Fig. 5h&k**), with reduced aspect ratios. Porous surface features and a high

aspect ratio facilitate dissolution media penetration (also entrapped media diffusion) and degree of swelling during the incubation period, which in this instance led to an enhanced release rate (Gao et al., 2015).

For most matrix type drug delivery systems diffusive mechanisms always appear to be the underlying mode of drug or active release (Gao et al., 2016). In order to propose a GLP release mechanism from composite particles the Korsmeyer-Peppas model was selected (Table 1) to evaluate *in vitro* release kinetics. The Korsmeyer-Peppas model is often applied where the *in vitro* release behavior is not well understood or a non-diffusive mechanism is likely. The Kormeyer-Peppas model is expressed as shown in Equation (6) (Korsmeyer et al., 1983):

$$M_t/M_\infty = kt^n \qquad \text{(Eq. 6)}$$

Here, M_t and M_∞ is the percentage of drug released at time t and infinite time ∞, respectively, k is a characteristic constant and n is the release exponent which indicates the release mechanism. A release exponent value below 0.45 indicates Fickian diffusion or case-I diffusion. When the n value is greater than 0.85, it indicates case-II diffusion, which contains certain interactions among drug molecules, release medium and the delivery matrix. When n value is in the range 0.45 to 0.85, an anomalous transport process is proposed, which involves multiple factors contributing towards the release mechanism (Peppas and Sahlin, 1989).

Model fit accuracy is usually demonstrated by high correlation coefficient values (R^2>0.95). The n values for the current study are 0.43, 0.34 and 0.33 for composite samples prepared at 25, 35 and 50 °C, respectively. This further confirms GLP release from all composite particles is *via* typical Fickian diffusion mechanism (all exponents

<0.45) (Yang et al., 2013). While this suggests changes to environmental temperature during ES operation has little to no influence on the GLP release mechanism, the increased *k* value for samples engineered at elevated temperatures (i.e. 16.00, 26.36, and 28.64 at 25, 35, and 50 °C, respectively) suggests particles could be engineered to tailor drug release as confirmed in **Fig. 8**.

4. Conclusion

GLP loaded NaAlg micro-particles with mean diameters ranging from 225 to 355 μm were successfully produced *via* the ES process to preserve the bioactive ingredient. The micro-particle size distribution was regulated by optimizing the concentration of collection medium ($CaCl_2$ solution) and processing parameters (flow rate, applied voltage and deposition distance) during electrospraying. In addition, changes to the environmental electrospraying temperature enabled particle shape and morphology variation. Transformation from conical to spherical geometries was observed, as a function of temperature, and crinkled surface topography became more prominent. FTIR analysis indicates the successful and stable encapsulation of GLP within NaAlg particle matrix, with little to no effect on the chemical structure integrity. Consistent values for GLP LC and EE within beads were obtained at all environmental electrospraying temperatures. GLP release varied based on particle morphology and surface topography, although the underlying mechanism for all was determined to be diffusive (Korsmeyer-Peppas model). The results indicate an auxillary ES method and its optimization to tailor composite particles for environmentally sensitive molecules (*via* encapsulation) especially for biomedical and pharmaceutical applications.

Acknowledgements

This work was financially supported by the Key Technologies R&D Program of

Zhejiang Province (2015C02035), the Fundamental Research Funds for the Central Universities, and the Research Fund for The Doctoral Program of Higher Education of China (20130101120170).

Reference:

Bhardwaj, N., Kundu, S.C., 2010. Electrospinning: A fascinating fiber fabrication technique. Biotechnol. Adv. 28, 325-347.

Casper, C.L., Stephens, J.S., Tassi, N.G., Chase, D.B., Rabolt, J.F., 2003. Controlling Surface Morphology of Electrospun Polystyrene Fibers: Effect of Humidity and Molecular Weight in the Electrospinning Process. Macromolecules 37, 573--578.

Chatterjee, S., Judeh, Z.M., 2015. Encapsulation of fish oil with N-stearoyl O-butylglyceryl chitosan using membrane and ultrasonic emulsification processes. Carbohydr. Polym. 123, 432-442.

Ekemen Z, Chang H, Ahmad Z, Bayram C, Rong Z, Denkbas EB, Stride E, Vadgama P, Edirisinghe M. 2011. Fabrication of biomaterials via controlled protein bubble generation and manipulation. Biomacromolecules 12(12):4291-300.

Fu, Y.J., Wei, L., Zu, Y.G., Shi, X.G., Liu, Z.G., Schwarz, G., Efferth, T., 2009. Breaking the spores of the fungus Ganoderma lucidum by supercritical CO2. Food Chem. 112, 71-76.

Gao, J., Li, W., Wong, S.P., Hu, M., Li, R.K.Y., 2014. Controllable morphology and wettability of polymer microspheres prepared by nonsolvent assisted electrospraying. Polymer 55, 2913-2920.

Gao, Y., Chang, M.W., Ahmad, Z., Li, J.S., 2016. Magnetic-responsive microparticles with customized porosity for drug delivery. Rsc Advances 6.

Gao, Y., Zhao, D., Chang, M.W., Ahmad, Z., Li, X., Suo, H., Li, J.S., 2015. Morphology control of electrosprayed core–shell particles via collection media variation. Mater. Lett. 146, 59-64.

Ghayempour, S., Mortazavi, S.M., 2013. Fabrication of micro–nanocapsules by a new electrospraying method using coaxial jets and examination of effective parameters on their production. J. Electrostatics 71, 717-727.

Hamid, Moghadam, Mohsen, Samimi, Abdolreza, Samimi, Mohamad, Khorram, 2008. Electro-spray of high viscous liquids for producing mono-sized spherical alginate beads. Particuology 6, 271-275.

Huang, X., Xiao, Y., Lang, M., 2012. Micelles/sodium-alginate composite gel beads: A new matrix for oral drug delivery of indomethacin. Carbohydr. Polym. 87, 790-798.

Iliescu, R.I., Andronescu, E., Ghitulica, C.D., Voicu, G., Ficai, A., Hoteteu, M., 2014. Montmorillonite-alginate nanocomposite as a drug delivery system--incorporation and in vitro release of irinotecan. Int. J. Pharm. 463, 184-192.

Jie, J., Xi, Z., Hu, Y.S., Yi, W., Wang, Q.Z., Li, N.N., Guo, Q.C., Dong, X.C., 2009. Evaluation of in vivo antioxidant activities of Ganoderma lucidum polysaccharides in STZ-diabetic rats. Food Chem. 115, 32-36.

Kamalian, N., Mirhosseini, H., Mustafa, S., Manap, M.Y., 2014. Effect of alginate and chitosan on viability and release behavior of Bifidobacterium pseudocatenulatum G4 in simulated gastrointestinal fluid. Carbohydrate Polymers 111, 700-706.

Kivelä, R., Henniges, U., Sontag-Strohm, T., Potthast, A., 2012. Oxidation of oat β-glucan in aqueous solutions during processing. Carbohydr. Polym. 87, 589-597.

Koo, S.Y., Cha, K.H., Song, D., Chung, D., Pan, C., 2014. Microencapsulation of peppermint oil in an alginate–pectin matrix using a coaxial electrospray system. Int. J. Food Sci. Tech. 49, 733–739.

Korsmeyer, R.W., Gurny, R., Doelker, E., Buri, P., Peppas, N.A., 1983. Mechanisms of solute release from porous hydrophilic polymers. International Journal of Pharmaceutics 15, 25-35.

Lazaridou, A., Biliaderis, C.G., 2007. Molecular aspects of cereal β-glucan functionality: Physical properties, technological applications and physiological effects. Journal of Cereal Science 46, 101-118.

Lee, Y.H., Mei, F., Bai, M.Y., Zhao, S., Chen, D.R., 2010. Release profile characteristics of biodegradable-polymer-coated drug particles fabricated by dual-capillary electrospray. Journal of Controlled Release 145, 58-65.

Li, Y., Ai, L., Yokoyama, W., Shoemaker, C.F., Wei, D., Ma, J., Zhong, F., 2013. Properties of Chitosan-Microencapsulated Orange Oil Prepared by Spray-Drying and Its Stability to Detergents. Journal of Agricultural & Food Chemistry 61, 3311-3319.

Ma, C.W., Feng, M., Zhai, X., Hu, M., You, L., Luo, W., Zhao, M., 2013. Optimization for the extraction of polysaccharides from Ganoderma lucidum and their antioxidant and antiproliferative activities. Journal of the Taiwan Institute of Chemical Engineers 44, 886-894.

Ma, H.T., Hsieh, J.F., Chen, S.T., 2015. Anti-diabetic effects of Ganoderma lucidum. Phytochemistry 114, 109-113.

Mckee, M.G., Wilkes, G.L., Colby, R.H., Long, T.E., 2004. Correlations of Solution Rheology with Electrospun Fiber Formation of Linear and Branched Polyesters. Macromolecules 37, 1760-1767.

Meng, F.L., Chian, K.S., Mhaisalkar, P.S., Ong, W.F., Ratner, B.D., 2009. Effect of electrospun poly(D , L -lactide) fibrous scaffold with nanoporous surface on attachment of porcine esophageal epithelial cells and protein adsorption. Journal of Biomedical Materials Research Part A 89A, 1040–1048.

Moomand, K., Lim, L.T., 2014. Oxidative stability of encapsulated fish oil in electrospun zein fibres. Food Res. Int. 62, 523-532.

Pan, K., Jiang, Q., Liu, G., Miao, X., Zhong, D., 2013. Optimization extraction of Ganoderma lucidum polysaccharides and its immunity and antioxidant activities. Int. J. Biol. Macromol. 55, 301-306.

Park CH, Min YK, Ji YY, Kim KH, Lee JC, Lee J. 2007. Preparation of Polymer/Drug Nano- and Micro-Particles by Electrospraying. Macromolecular Symposia 249-250(1):116-9.

Park, H.K., Pyung-Hwan; Hwang, Waewon; Kwon, Oh-Joon; Park, Tae-Joon; Choi, Sung-Wook; Yun, Chae-Ok; Kim, Jung Hyun, 2012. Fabrication of cross-linked alginate beads using electrospraying for adenovirus delivery. Int. J. Pharm. 427, 417-425.

Peppas, N.A., Sahlin, J.J., 1989. A simple equation for the description of solute release. III. Coupling of diffusion and relaxation. International Journal of Pharmaceutics 57, 169-172.

Qin, S.S., Wun, L.H., 2002. A Rapid Method for Detecting Ganoderma Lucidum of Six Colors by FTIR Spectroscopy. Spectroscopy & Spectral Analysis 22, 226-228.

Qiu, X., Leporatti, S., Edwin Donath, † And, Möhwald, H., 2001. Studies on the Drug Release Properties of Polysaccharide Multilayers Encapsulated Ibuprofen Microparticles. Langmuir 17, 5375-5380.

Ribeiro, C.C., Barrias, C.C., Barbosa, M.A., 2004. Calcium phosphate-alginate microspheres as enzyme delivery matrices. Biomaterials 25, 4363-4373.

Shi, L.E., Li, Z.H., Li, D.T., Xu, M., Chen, H.Y., Zhang, Z.L., Tang, Z.X., 2013. Encapsulation of probiotic Lactobacillus bulgaricus in alginate–milk microspheres and evaluation of the survival in simulated gastrointestinal conditions. Journal of Food Engineering 117, 99–104.

Shi, M., Zhang, Z., Yang, Y., 2013. Antioxidant and immunoregulatory activity of Ganoderma

lucidum polysaccharide (GLP). Carbohydr. Polym. 95, 200-206.
Siepmann, J., Peppas, N.A., 2011. Higuchi equation: Derivation, applications, use and misuse. International Journal of Pharmaceutics 418, 6-12.
Suksamran, T., Ngawhirunpat, T., Rojanarata, T., Sajomsang, W., Pitaksuteepong, T., Opanasopit, P., 2013. Methylated N-(4-N,N-dimethylaminocinnamyl) chitosan-coated electrospray OVA-loaded microparticles for oral vaccination. International Journal of Pharmaceutics 448, 19-27.
Suksamran, T., Opanasopit, P., Rojanarata, T., Ngawhirunpat, T., Ruktanonchai, U., Supaphol, P., 2009. Biodegradable alginate microparticles developed by electrohydrodynamic spraying techniques for oral delivery of protein. Journal of Microencapsulation 26, 563-570.
Teng, B.S., Wang, C.D., Zhang, D., Wu, J.S., Pan, D., Pan, L.F., Yang, H.J., Zhou, P., 2012. Hypoglycemic effect and mechanism of a proteoglycan from ganoderma lucidum on streptozotocin-induced type 2 diabetic rats. European Review for Medical & Pharmacological Sciences 16, 166-175.
Wang, J., Zhang, L., Yu, Y., Cheung, P.C.K., 2009. Enhancement of Antitumor Activities in Sulfated and Carboxymethylated Polysaccharides of Ganoderma lucidum. Journal of Agricultural & Food Chemistry 57, 10565-10572.
Wang, X., Chen, X., Qi, Z., 2012. A study of Ganoderma lucidum spores by FTIR microspectroscopy. Spectrochimica Acta Part A Molecular & Biomolecular Spectroscopy 91, 285-289.
Wee, S., Gombotz, W.R., 1998. Protein release from alginate matrices. Adv. Drug Del. Rev. 31, 267-285.
Wu, Y., Clark, R.L., 2007. Controllable porous polymer particles generated by electrospraying. Journal of Colloid & Interface Science 310, 529-535.
Yang, J.M., Zha, L.S., Yu, D.G., Liu, J., 2013. Coaxial electrospinning with acetic acid for preparing ferulic acid/zein composite fibers with improved drug release profiles. Colloids & Surfaces B Biointerfaces 102, 737-743.
Yao, Z.C., Chang, M.W., Ahmad, Z., Li, J.S., 2016a. Encapsulation of rose hip seed oil into fibrous zein films for ambient and on demand food preservation via coaxial electrospinning. J. Food Eng. 191, 115-123.
Yao, Z.C., Gao, Y., Chang, M.W., Ahmad, Z., Li, J.S., 2016b. Regulating poly-caprolactone fiber characteristics in-situ during one-step coaxial electrospinning via enveloping liquids. Mater. Lett. 183, 202-206.
Yuan, G., Ding, Z., Chang, M.W., Ahmad, Z., Li, J.S., 2016. Optimising the shell thickness-to-radius ratio for the fabrication of oil-encapsulated polymeric microspheres. Chem. Eng. J. 284, 963-971.
Zhang, J., Gao, X., Pan, Y., Xu, N., Jia, L., 2016. Toxicology and immunology of Ganoderma lucidum polysaccharides in Kunming mice and Wistar rats. Int. J. Biol. Macromol. 85, 302-310.
Zhao, D., Li, J.S., Suen, W., Chang, M.W., Huang, J., 2016. Preparation and characterization of Ganoderma lucidum spores-loaded alginate microspheres by electrospraying. Materials Science & Engineering C Materials for Biological Applications 62, 835-842.

Table and Figure Captions

Tables

Table 1. Korsmeyer-Peppas model applied to GLP release kinetics from composite particles

Figures

Figure 1. (a) Schematic diagram of the electrospray (ES) set-up. In-sets exhibit characteristic ES modes at selected applied voltages: (b) dripping mode ~0 kV; (c) stable-jet mode ~15 kV.

Figure 2. Optical micrographs of NaAlg particles collected using $CaCl_2$ solutions with variable concentrations: (a) 0 w/v%; (b) 0.5 w/v%; (c) 1 w/v%; (d) 2 w/v%; (e) 5 w/v%; (f) 10 w/v%; (g) 20 w/v%. (h) NaAlg particle diameter distribution (collected in various $CaCl_2$ solutions).

Figure 3. Effect of ES processing parameters on resulting NaAlg and NaAlg/GLP particle diameters: (a) Flow rate-NaAlg; (b) Flow rate-NaAlg/GLP; (c) Applied voltage-NaAlg; (d) Applied voltage-NaAlg/GLP; (e) Collection distance-NaAlg; (f) Collection distance-NaAlg/GLP.

Figure 4. Optical micrographs of NaAlg/GLP particles prepared at different environmental temperatures: (a) 25 °C; (c) 35 °C; (e) 50 °C. (b, d, &f) show NaAlg/GLP particle diameter distributions for (a, c, &e) environments, respectively.

Figure 5. Electron micrographs of alginate particles prepared at various

environmental temperatures: (a) NaAlg particles-25 °C; (d) NaAlg/GLP particles-25 °C; (g) NaAlg/GLP particles-35 °C; (j) NaAlg/GLP particles-50 °C. In-sets at top right corner in (a, d, g, &j) are high-magnification images. (b, e, h, &k) are magnified images providing greater surface details for (a, d, g, &j), respectively. Schematic diagrams for resulting particles: (c) NaAlg particles-25 °C; (f) NaAlg/GLP particles-25 °C; (i) NaAlg/GLP particles-35 °C; (l) NaAlg/GLP particles-50 °C.

Figure 6. FTIR spectra of raw materials and particle systems prepared in the study.

Figure 7. GLP loading capacity (LC) and encapsulation efficiency (EE) within NaAlg matrix at various environmental temperatures (N.S.=no significant difference).

Figure 8. GLP Release profiles from NaAlg/GLP particles prepared at various environmental temperatures in simulated GI tract environments (SGF and SIF).

Tables

Table 1

Sample	Korsmeyer-Peppas model	k	n	R^2
25°C NaAlg/GLP	$\log(M_t/M_\infty \times 100)=1.20+0.43\times\log(t)$	16.00	0.43	0.9550
35°C NaAlg/GLP	$\log(M_t/M_\infty \times 100)=1.42+0.34\times\log(t)$	26.36	0.34	0.9558
50°C NaAlg/GLP	$\log(M_t/M_\infty \times 100)=1.46+0.33\times\log(t)$	28.64	0.33	0.9599

Figures

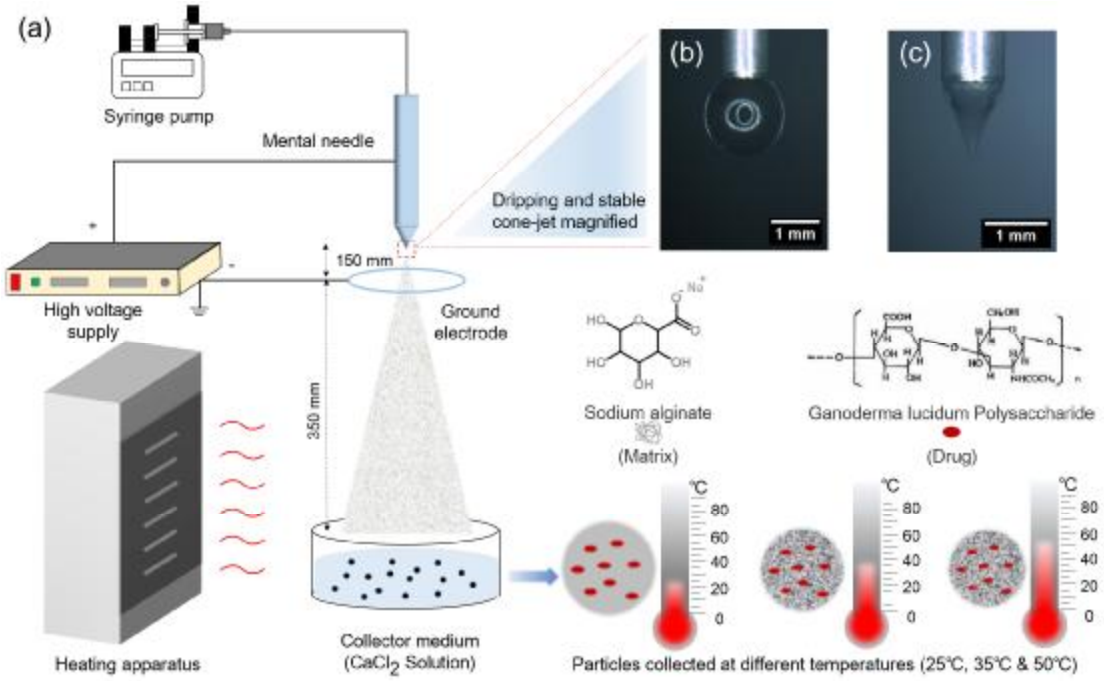

Figure 1

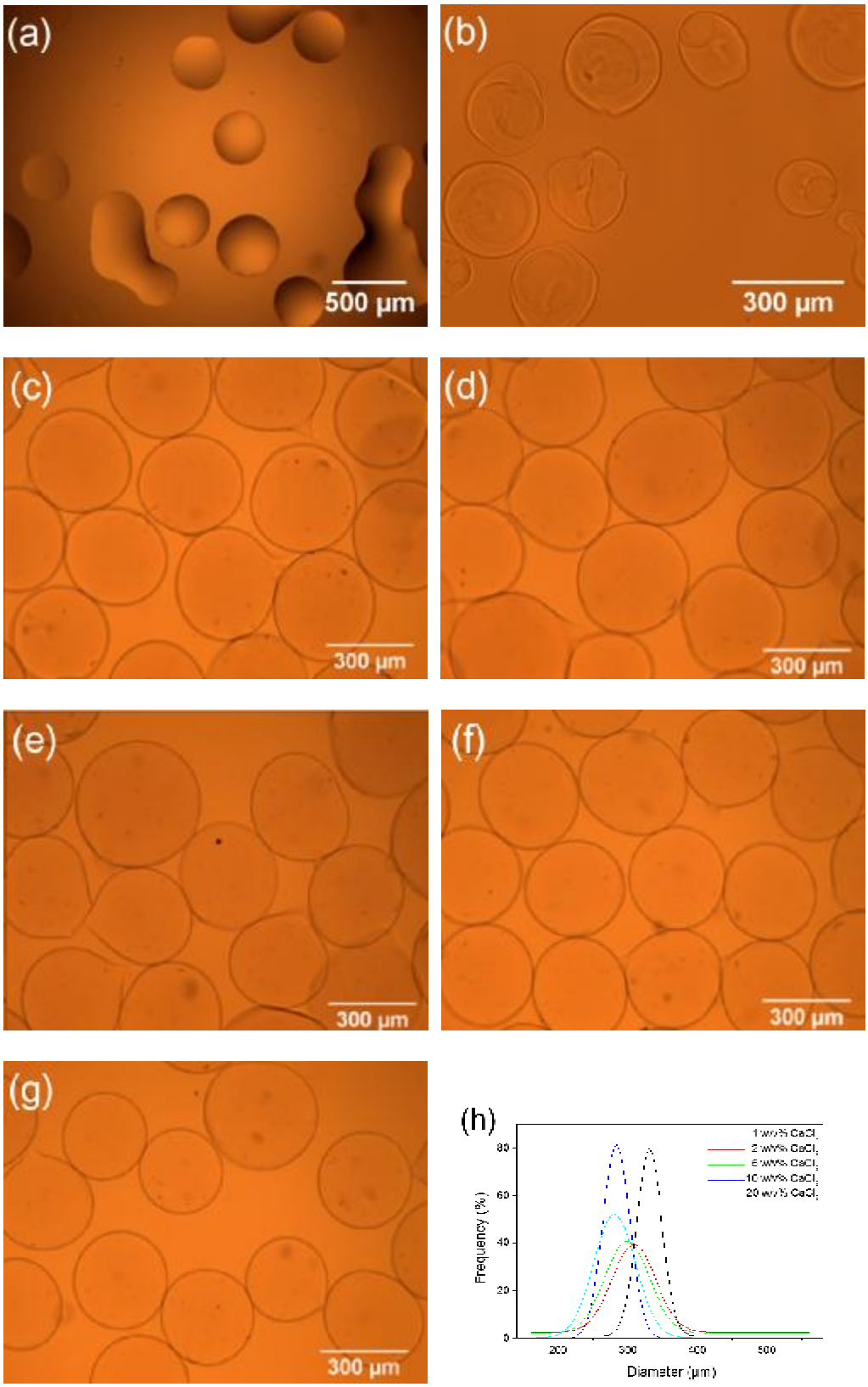
(a)
500 µm
(b)
300 µm
(c)
300 µm
(d)
300 µm
(e)
300 µm
(f)
300 µm
(g)
300 µm
(h)
Frequency (%)
Diameter (µm)

Figure 2

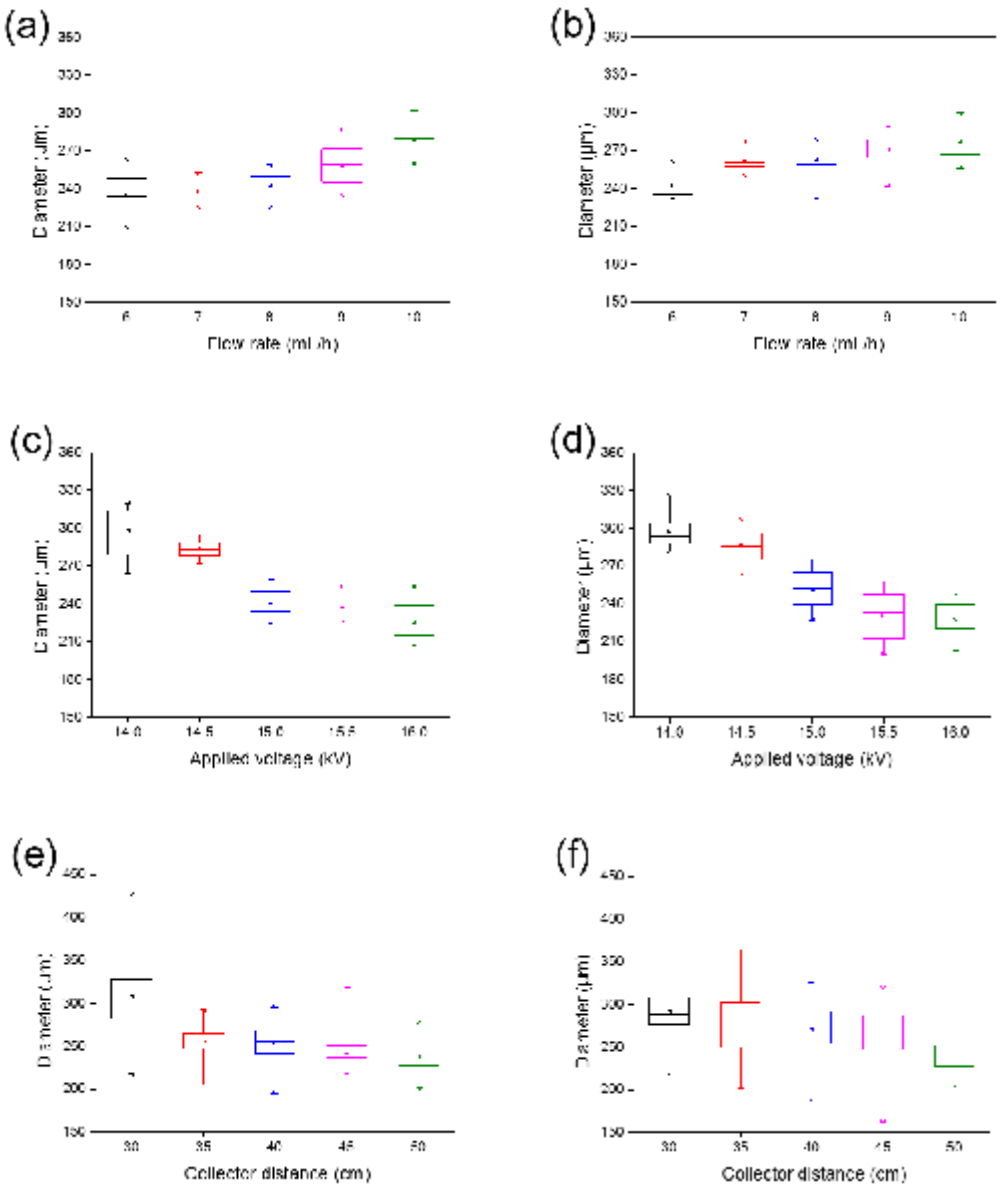
(a)
Diameter (μm)
Flow rate (ml /h)
(b)
Diameter (μm)
Flow rate (ml /h)
(c)
Diameter (μm)
Applied voltage (kV)
(d)
Diameter (μm)
Applied voltage (kV)
11.0
14.5
15.0
15.5
18.0
(e)
Diameter (μm)
Collector distance (cm)
(f)
Diameter (μm)
Collector distance (cm)

Figure 3

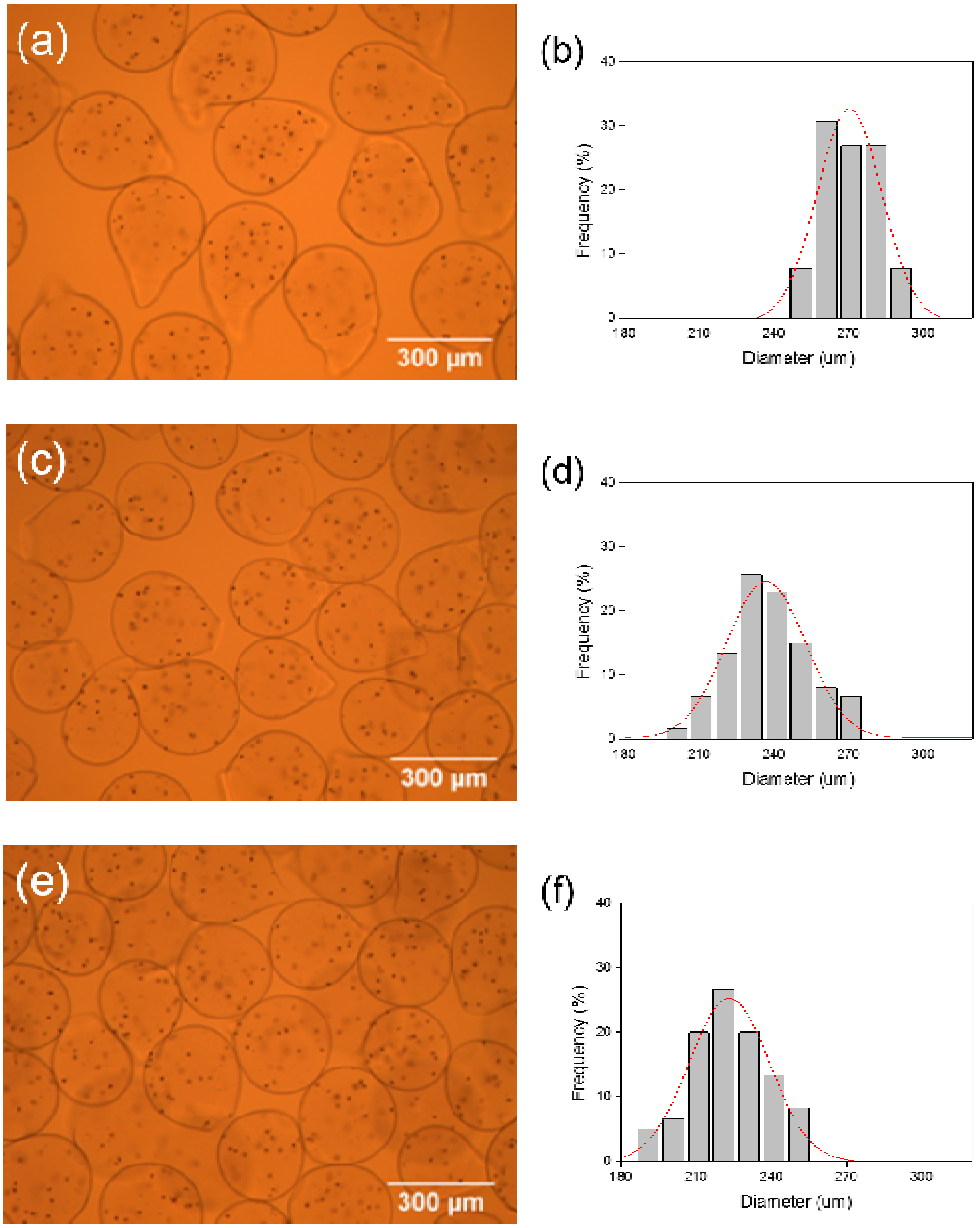
(a)
300 µm
(b)
Frequency (%)
Diameter (um)
(c)
300 µm
(d)
Frequency (%)
Diameter (um)
(e)
300 µm
(f)
Frequency (%)
Diameter (um)

Figure 4

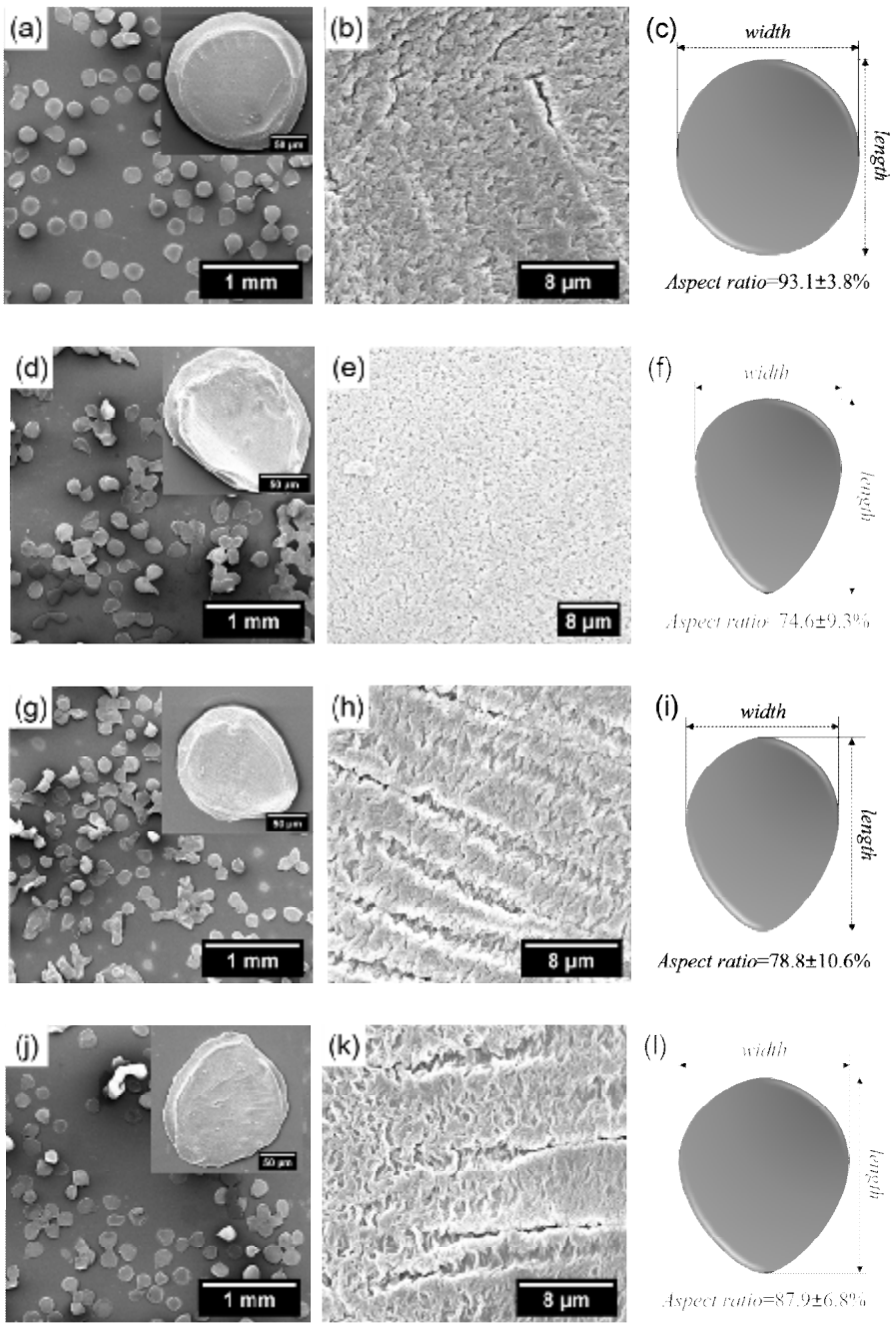
(a)
1 mm
(b)
8 µm
(c)
width
length
Aspect ratio=93.1±3.8%
(d)
1 mm
(e)
8 µm
(f)
width
length
Aspect ratio=74.6±9.3%
(g)
1 mm
(h)
8 µm
(i)
width
length
Aspect ratio=78.8±10.6%
(j)
1 mm
(k)
8 µm
(l)
width
length
Aspect ratio=87.9±6.8%

Figure 5

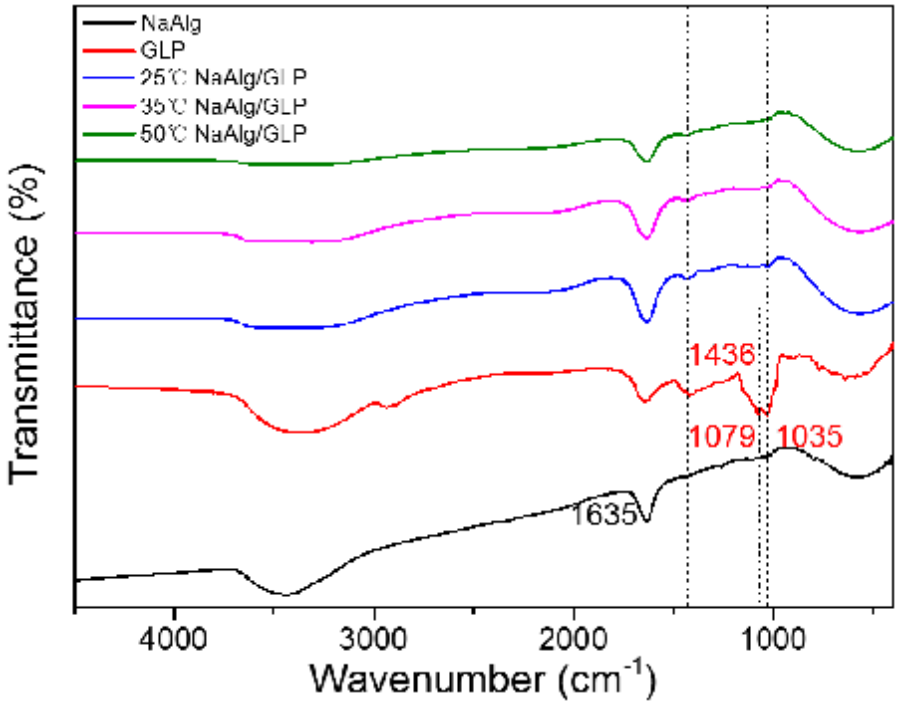

Figure 6

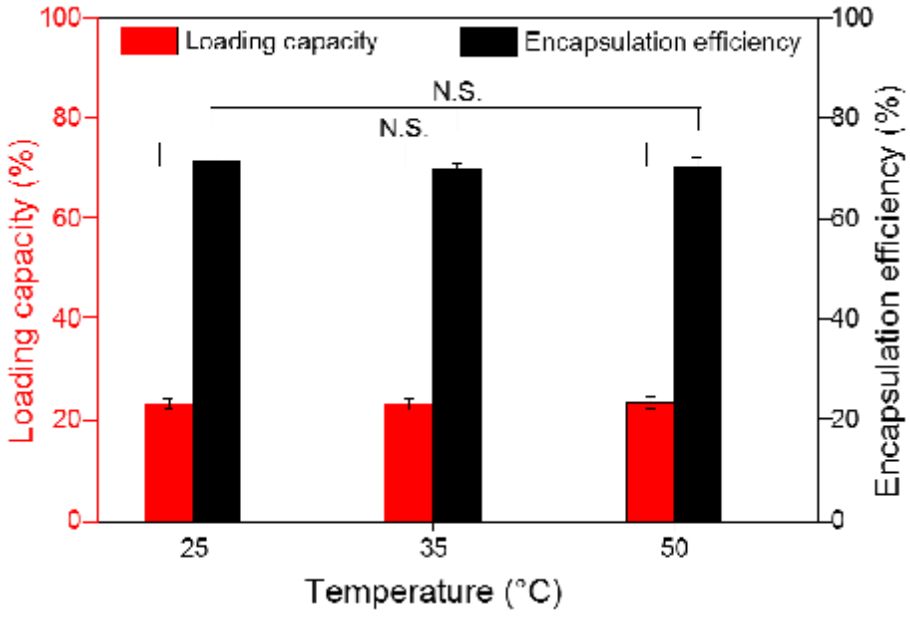

Figure 7

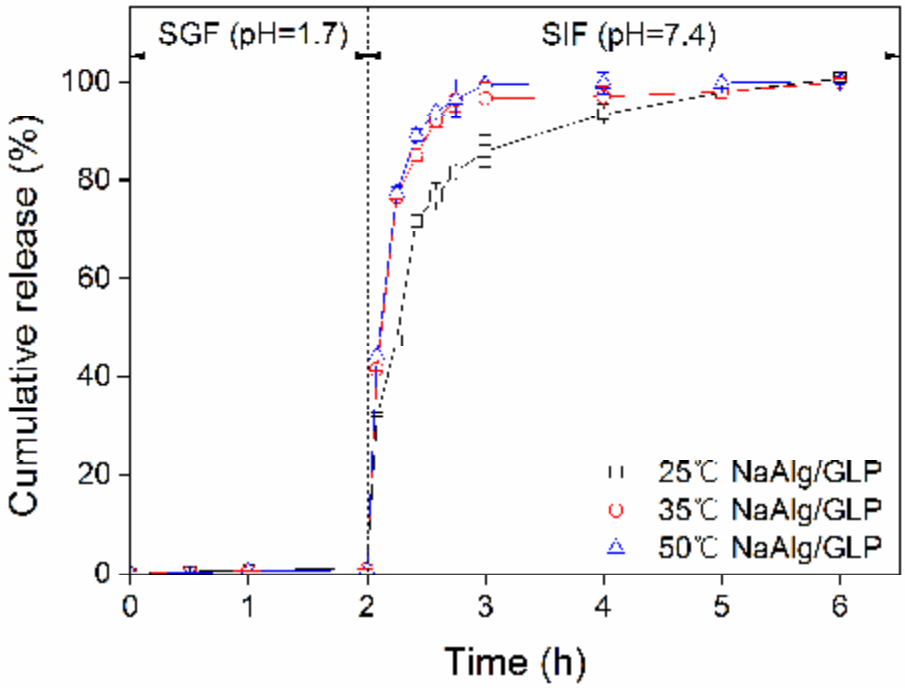
SGF (pH=1.7)
SIF (pH=7.4)
Cumulative release (%)
Time (h)
25℃ NaAlg/GLP
35℃ NaAlg/GLP
50℃ NaAlg/GLP
0
20
40
60
80
100
0
1
2
3
4
5
6

Figure 8